research articles Journal of proteome research

Integrative Study on Proteomics, Molecular Physiology, and Genetics Reveals an Accumulation of Cyclophilin-Like Protein, TaCYP20-2, Leading to an Increase of Rht Protein and Dwarf in a Novel GA-Insensitive Mutant (*gaid*) in Wheat

Beibei Li,[†,‡,§] Wenzhong Xu,[†,‡] Yunyuan Xu,[‡] Yuanyuan Zhang,[‡,§] Tai Wang,[‡] Yue Bai,[‡] Chenggui Han,[∥] Aimin Zhang,[⊥] Zhihong Xu,[‡] and Kang Chong*[,‡]

Research Center for Molecular Developmental Biology, Key Lab of Photosynthesis and Environmental Molecular Physiology, Institute of Botany, CAS, Beijing 100093, China, College of Biology, China Agricultural University, Beijing 100193, China, Institute of Genetics and Developmental Biology, CAS, Beijing 100101, China, and Graduate University of the Chinese Academy of Sciences, Beijing 100049, China

Received June 5, 2010

Dwarfism with a "Green Revolution" phenotype is a desirable agronomic trait for crop cultivators as associated with increased yield, improved lodging resistance and higher fertility. Few dwarf mutants of hexaploid wheat (*Triticum aestivum*), except for *Rht-B1* and *Rht-D1*, have been identified. Here, we report on a novel dwarf natural wheat mutant, which is identified as a gibberellic acid (*GA*)-*i*nsensitive *d*warf (*gaid*) mutant for its semidominant blocking GA signaling pathway. Physiological and morphological investigations showed that the shoot elongation of *gaid* mutant plants is insensitive to exogenous GA_3 treatment. Expression of *TaGA20ox1* in the *gaid* mutant was enhanced after GA_3 treatment. The short stem of *gaid* resulted from reduced cell elongation. The transcript expression of *Rht*, encoding a DELLA protein negatively regulating GA signaling in wheat, displayed similar patterns between *gaid* and wild type. Contrarily, the degradation of Rht induced by GA_3 treatment was suppressed in the mutant. 2-DE screening assay showed that the expression patterns of the mutant, as well as their responses to GA_3, were changed as compared with the wild type. In the mutant, one of enriched proteins was identified as TaCYP20-2 by Q-TOF MS approach and immunoblotting. TaCYP20-2 was localized in the chloroplast and cell plasma membrane. The transcript of *TaCYP20-2* was higher in *gaid* than that in wild type. Molecular genetic data showed that overexpression of *TaCYP20-2* in wheat resulted in a dwarfism similar to that of *gaid*. It suggests that TaCYP20-2 is a new member that regulates wheat stem development mediated by DELLA protein degradation of GA signaling pathway.

Keywords: dwarf mutant *gaid* • gibberellin • proteomics • cyclophilin • DELLA protein • *Triticum aestivum* (wheat)

1. Introduction

Since the 1960s, agriculture has developed new varieties of grain crops with short stems and cultivation, the "Green Revolution", to substantially increase crop yields.[1] Dwarfism is a desirable characteristic for grain crops breeding. Dwarf varieties are more resistant to the damaging effects of wind and rain that cause stem lodging.[2] Therefore, dwarf cereal is usually considered as a potential variety for increasing grain production with a less expense of biomass.

Dwarfism is commonly caused by mutations in genes regulating the biosynthesis or the signaling transduction of plant hormone gibberellic acid (GA). Various dwarf mutants in *Arabidopsis* (*Arabidopsis thaliana*; *ga1-3* and *gai*), maize (*Zea mays*; *d8*), rice (*Oryza sativa*; *sd1* and *slr1*), barley (*Hordeum vulgare*; *sln1*), and wheat (*Triticum aestivum*; *Rht-B1* and *Rht-D1*) have been characterized and classified as being deficient or insensitive to the plant hormone GA.[3−9] Mutants severely defective in GA biosynthesis, such as the *Arabidopsis* mutant *ga1-3*, contain extremely low levels of bioactive GA and cannot germinate without GA treatment. The *ga1-3* is a null gene encoding *ent*-copalyl diphosphate synthase in an early step of the GA biosynthesis pathway,[9] so that the GA-deficient phenotypes of the *ga1-3* mutant can be rescued by application of exogenous GA_3. Besides, rice semidwarf *sd1* mutant which contains a defective gibberellin 20-oxidase gene has a phenotype similar to *ga1-3*.[8]

GAI, *D8*, *SLR1*, *SLN1*, and *Rht* encode members of the DELLA subfamily within the GRAS family of plant regulatory proteins, which negatively regulate GA signaling transduction. Truncated

* To whom correspondence should be addressed. Fax +86 10 82594821; e-mail chongk@ibcas.ac.cn.
† These authors contributed equally to this work.
‡ Institute of Botany, CAS.
§ Graduate University of the Chinese Academy of Sciences.
∥ China Agricultural University.
⊥ Institute of Genetics and Developmental Biology, CAS.

Published on Web 06/08/2010
10.1021/pr100560v

mutations of *GAI*/*D8*/*SLR1*/*Rht* in the N terminal of DELLA proteins display a GA-insensitive response and gain the function to constitutively repress GA signaling.[3,4,10,11] These dominant dwarf mutants fail to grow rapidly in response to GA treatment, but can be further dwarfed by GA biosynthesis inhibitor. In contrast to GA-insensitive phenotype in the gain-of-function mutants, loss-of-function mutants of barley *sln1* and rice *slr1* show a constitutive GA response phenotype with an elongated stem and leaf.[6,12] Other dwarf GA-insensitive mutants are the *repression of shoot growth* (*rsg*) in tobacco (*Nicotiana tabacum* L.), *photoperiod-responsive1* (*phor1*) in potato (*Solanum tuberosum*), *dwarf1* (*d1*) and *GA-insensitive dwarf1* (*gid1*) in rice.[13−16] The proteins including RSG, PHOR1, D1, and GID1 function as positive regulators of GA signaling. GID1 is a soluble receptor mediating GA signaling in rice and shares sequence similarity with a hormone-sensitive lipase (HSL).[15,17] The double mutant of *gid1* and *slr1* shows *GID1* acting upstream of *SLR1* in the GA signaling pathway, and SLR1 as a DELLA protein in rice was not degraded in the *gid1* mutant on treatment with GA. The GA-insensitive dwarf mutants *sleepy1* (*sly1*) in *Arabidopsis* and *GA-insensitive dwarf2* (*gid2*) in rice revealed new insight into the GA signaling pathway. The SLY1 and GID2 proteins, which are homologous F-box proteins as a subunit of the SCF (Skp1/cullin/F-box) E3 ligase complex promote GA-dependent degradation of DELLA proteins in the ubiquitin proteasome pathway.[18,19] Binding GA with GID1 induces the interaction between the DELLA proteins and GID1 and the degradation of DELLA proteins mediated by the F-box protein.[17]

Immunophilins consist of two subfamilies, cyclophilins and FK506-binding proteins (FKBPs). The members of the cyclophilin family appear in all kinds of species such as bacteria, fungi, insects, plants and animals, and are present in all subcellular compartments.[20] The cyclophilin family modulates diverse processes, including protein folding, protein degradation, mRNA processing, apoptosis, development, stress responsiveness and receptor signaling. Moreover, the expression of cyclophilin is induced by both biotic and abiotic stresses.[21] The plant cyclopilins were identified in the 1990s in diverse crops such as tomato (*Lycopersicon esculentum*), maize and oilseed rape (*Vitis vinifera*).[22] They consist of a wide variety of single and multidomain isoforms varying by cellular locations and functions but mainly focus on participating in photosynthesis in chloroplasts and regulation of plant development.[21] For example, TLP20, the spinach (*Spinacia oleracca*) cyclophilin protein, is the major peptidyl-prolyl cis−trans isomerase (PPIase) and protein-folding catalyst in the thylakoid lumen.[23] The multidomain spinach cyclophilin TLP40 can be associated with PSII-specific protein phosphatase within the thylakoid membrane and regulate its activity, which is an essential process coinciding with phosphatase activation and dephosphorylation of PSII reaction center proteins.[24,25] A few reports in the literature revealed the relationship between immunophilin-type PPIase and cell elongation. The *Arabidopsis FKBP42* loss-of-function *mutant twisted dwarf1* (*twd1*) displays a drastic reduction of cell elongation combined with a disoriented growth behavior of all plant organs.[26] Lacking a cyclophilin, CYP40, causes a defect in the transition from the juvenile to adult stages of vegetative development and inflorescence morphology in *Arabidopsis*.[27] Mutations in *PAS1* (*AtFKBP70*) leading to tumor growth in plants indicates that *FKBP70* is required for correct cell division and cell differentiation.[28] CYP71 regulates plant morphogenesis and serves as a histone remodeling factor involved in chromatin-based silencing.[29]

Wheat is an important cereal crop with a complex hexaploid background (approximately 17 000 Mb), which causes difficulties in genomic mutation, gene cloning and genomic modification. The transcriptome analysis of gene expression at the mRNA level has contributed greatly to characterizing mutants of *Arabidopsis* and rice. In contrast, obstacles exist in studying the gene expression of wheat. Moreover, the level of mRNA does not always correlate well with the level of protein, the key player in the cell, as a result of post-transcriptional regulation mechanism. Therefore, proteome studies aiming at the complete set of genome-encoded proteins may complement the shortages of the transcriptome approaches. Here, we provide a successful explore using integrative studies of proteomics, physiology and molecular genetics to resolve the mutant with complex genetic background. We screened and characterized a new dwarf wheat mutant named as *gaid* (*GA-i*nsensitive *d*warf) which was insensitive to GA. Proteomics approaches can provide new insights into the dwarfism of the *gaid* wheat mutant. Our comparative proteomic analysis identified the accumulation of a cyclophilin protein, TaCYP20-2, in dwarf wheat. The transgenic wheat plants with *TaCYP20-2* overexpression show a reduced height phenotype similar to the *gaid* mutant. The novel mechanism provides a new way to create a dwarf wheat cultivar for agricultural applications.

2. Materials and Methods

2.1. Isolation of *gaid* Wheat Mutant. A dominant dwarf wheat mutant was screened from the progenies of a transgenic wheat line (background *Triticum aestivum* cv. Jingdong 1) by the pollen tube transformation method.[30,31] It was named as *gaid*, a GA-insensitive dwarf because of its physiological response. Experiments showed this mutation irrelevant to the foreign DNA sequence and relevant to natural mutagenesis. The *gaid* wheat seeds used in the experiments were the fifth generation of the origin mutant, which showed stable genetic characters. Local cultivars of winter wheat as hybrid parents, such as DN3214, ND99−5009, Jing411, and BAU3338 were crossed with *gaid*.

2.2. Plant Materials and Growth Conditions. In field experiments, wild-type and *gaid* seeds were sown in the fall. In the following spring, the seedlings were sprayed with or without 100 μM GA_3 (Sigma, St. Louis, MO, USA) for 4 weeks.

To investigate the role of GA_3 and paclobutrazol (PAC) in leaf sheath elongation, seeds were surface-sterilized for 20 min with a 2% NaClO solution, washed with water and then placed on moistened papers for germination. After the seeds germinated for 2 days, seedlings with a uniform shoot length for the wild type and *gaid* mutants were selected (providing 30 seedlings per sample) and transferred to solution media, 1/2 Murashige and Skoog medium (pH 5.2), with the appropriate concentration of GA_3 and PAC. The hydroponic medium was replaced with a new solution once every 3 days. Thirteen days later, the first leaf sheath length was determined in both the wild type and *gaid*.

2.3. Imaging of Leaf Sheath Cell Size. To examine cell arrangement and size, 5-mm-long fragments of the first leaf sheath apex of 7-day-old wheat seedlings were incubated in FAA buffer (10% glacial acetic acid, 10% 40% formalin, 80% 70% alcohol) for 48 h, then transferred into DL-lactic acid for 24 h. The length of epidermal cells in the leaf sheath was measured

by use of a differential interference contrast (DIC) microscope (Zeiss) at 10× magnification.[32]

2.4. Semiquantitative PCR and Quantitative Real-time PCR. Total RNA was extracted from shoots of 15-day-old of wild-type and *gaid* seedlings by use of Trizol reagent (Invitrogen, Carlsbad, CA). cDNA was generated using the Reverse Transcriptase kit (TaKaRa, Tokyo, Japan). The primer pairs used for semiquantitative RT-PCR were as follows: for *Rht-D1a*, 5′-ATG AAG CGG GAG TAC CAG GAC G-3′ and 5′-CAT GCC GAG GTG GCG ATC AGC-3′ and for *TaCYP20-2*, 5′-ATGGCGGCCGC-GACCTCCT-3′ and 5′- TCAGACCACTGGAAGCTCCCC-3′. As a control, a fragment from the gene that encodes *T. aestivum* alpha-tubulin was amplified by means of the primers 5′-CGT CGA CAG GCG TCT TCG TAC T-3′ and 5′-CAA GGA GTG AGT GGG TGG ACA GGA C-3′. RT-PCR reactions were repeated five times.

For real-time PCR, 2 μg of total RNA was used for RT with SuperScripts II reverse transcriptase (Invitrogen). The cDNA samples were diluted to 2 to 8 ng/μL. Triplicate quantitative assays were performed on 5 μL of each cDNA dilution with the SYBR Green PCR Master mix (TaKaRa) and an Mx3000P sequence detection system (STRATAGENE) according to the manufacturer's protocol (Applied Biosystems). The relative quantification method (Delta−Delta CT) was used to evaluate quantitative variation between the replicates examined. The amplification of *T. aestivum Tubulin* was used as an internal control to normalize all data, primers for *Tubulin* were 5′-TGTGCCCCGTGCTGTTCTTATG-3′ and 5′-CCCTTGGCCCAGT-TGTTACCC-3′. Gene-specific primers for *Rht-D1a* (GenBank: AJ242531) were 5′-GTTCGAGACCGTCCACCTGG-3′ and 5′-CATGCCGAGGTGGCGATCAGC-3′; for *TaCYP20-2* (GenBank: AY217753), 5′-ACGGTCAAGACACCGTGGCTG-3′ and 5′- TCA-GACCACTGGAAGCTCCCC-3′; for *TaGA20ox1* (GenBank: Y14008), 5′-ATGGTGCAGCCGGTGTTCGACG-3′ and 5′-GCATGCCGC-CGATGTCGA TGAG-3′.

2.5. Protein Sample Preparation and 2D Gel Analysis. Protein was extracted from aerial part of seedlings of *gaid* and wild type at 15 day from germination with 9 M urea, 2% CHAPS, 1% DTT and 2% Pharmalyte 3−10, following the method described for 2D electrophoresis manuscript (2D; GE Healthcare). Isoelectric focusing (IEF) for the first dimension was carried out using 24-cm-long IPG strips (GE Healthcare) with a linear pH gradient from 3 to 10. Each sample (600 μg) was mixed with the IEF sample buffer underwent the following steps: 12-h rehydration at 20 °C, 1-h 500 V, 1-h 1000 V, then 8.5-h 8000 V. Intensity was limited to 50 μA/strip. Equilibration of IPG strips was as previously described (GE Healthcare). The first equilibration was performed in a solution containing 6 M urea, 50 mM Tris-HCl, pH 8.8, 30% (v/v) glycerol, 2% (w/v) SDS, and 0.002% (w/v) bromophenol blue, with 1% (w/v) DTT. The second equilibration was as the first equilibration except that DTT was replaced with 2.5% (w/v) iodoacetamide. SDS-PAGE was carried out at 7 W/gel by use of 12% polyacrylamide gels as described.[33] Gels were stained overnight with Coommassie brilliant blue (CBB) G-250. The experiment involved three replicated gels.

2.6. Image and Data Analysis. The CBB-stained gels were scanned on a flatbed scanner (GE healthcare) at 300 dpi resolution. Detection, quantification, and matching of differentially displayed protein spots involved use of ImageMaster 5.0 2D Platinum image software (GE Healthcare). The wild-type and *gaid* images were compared for 2-DE patterns of protein spots by examining the spot intensity and calculating relative spot volume (%Vol). Only spots showing significant changes between the wild-type and *gaid* samples (%Vol varied more than 2-fold) were selected for further identification.

2.7. In-Gel Digestion and Mass Spectrometry. All of the differentially expressed spots were manually excised from the 2-DE gels. In-gel digestion and mass spectrometry (MS) acquisition were performed as described.[34] The MS spectra were created by use of quadrupole time-of-flight MS (Q-TOF MS; Micromass) equipped with a z-spray source. Tandem MS data were processed by use of MaxEnt 3.0 (Micromass) to create peak lists. The MASCOT version 2.1 search engine (www.matrixscience.com) was used for protein identification by the peptide mass fingerprint search of the National Center for Biotechnology Information (NCBI) database. Carbamidomethyl (C), oxidation (M) and pyro-glu (N-term Q) were set as a fixed modification.

2.8. Immunoblotting. The polyclonal TaCYP20-2 antisera was produced as described.[35] *TaCYP20-2* was amplified for the construction of the prokaryotic expression vector by primers (5′-CGGATCCATGGCGGCCGCGACCTC-3′ and 5′-CGGAATTCTCAGACCACTGGAAGCTCC-3′). The recombined plasmid pGEX4T-1-*TaCYP20-2* was transformed into *Escherichia coli* DH5α cells. Polyclonal antisera were raised by subcutaneously inoculating New Zealand white rabbits with about 2.5 mg of recombinant proteins emulsified in an equal volume of Freund's adjuvant.

IEF for the first dimension was carried out using 7-cm-long IPG strips (GE Healthcare) with a linear pH gradient from 3 to 10. Total proteins were separated by 12% SDS-PAGE and transferred to PVDF membrane. TaCYP20-2 protein was detected by anti-TaCYP20-2 polyclonal antibody. Rht protein was detected by polyclonal antibody raised against the conserved N-terminal domains (DELLA domain and TVHYNPS domain) of barley SLN1. SLN1 from barley is an ortholog of Rht, and has 92% identity with Rht. The α-tubulin polyclonal antibody (Beyotime) was used to detect tubulin protein as loading control.

2.9. Localization of TaCYP20-2-Green Fluorescent Protein (GFP) Fusion Protein. The whole coding sequence of *TaCYP20-2* amplified with two primers (5′-TCTAGAATGGCGGC-CGCGACCTCC-3′ and 5′-GGTACCGACCACCGG AAGCTCCCCG-3′) was cloned into the *Xba*I-*Kpn*I sites of the pBI121 vector to generate pBI121-*TaCYP20-2-GFP* containing a *TaCYP20-2-GFP* fusion construct under the control of cauliflower mosaic virus 35S (CaMV 35S) promoter. This construct was electroporated into *Agrobacterium tumefaciens* C58 and transformed into *Arabidopsis* by the floral dip method as described.[36]

Seeds from plants transfected with pBI121-*TaCYP20-2-GFP* vector were screened on selection medium (1/2 Murishige and Skoog medium, 50 μg/mL kanamycin). The T2 generation was used for further experiments. GFP fluorescence was excited at 488 nm by use of a Confocal microscope (ZEISS LSM 510 META, Zeiss) and detected with 510−550- and 635−680-nm filters.

Leaves from *TaCYP20-2-GFP* transgenic *Arabidopsis* were cut into 0.5−1-mm strips with the use of fresh razor blades without wounding. Leaf strips were put in a Petri dish with an enzyme solution (1−1.5% cellulose R10, 0.2−0.4% macerozyme R10, 0.4 M mannitol, 20 mM KCl, 20 mM MES, pH 5.7) and digested for another 60 to 90 min with gentle shaking (40 rpm on a

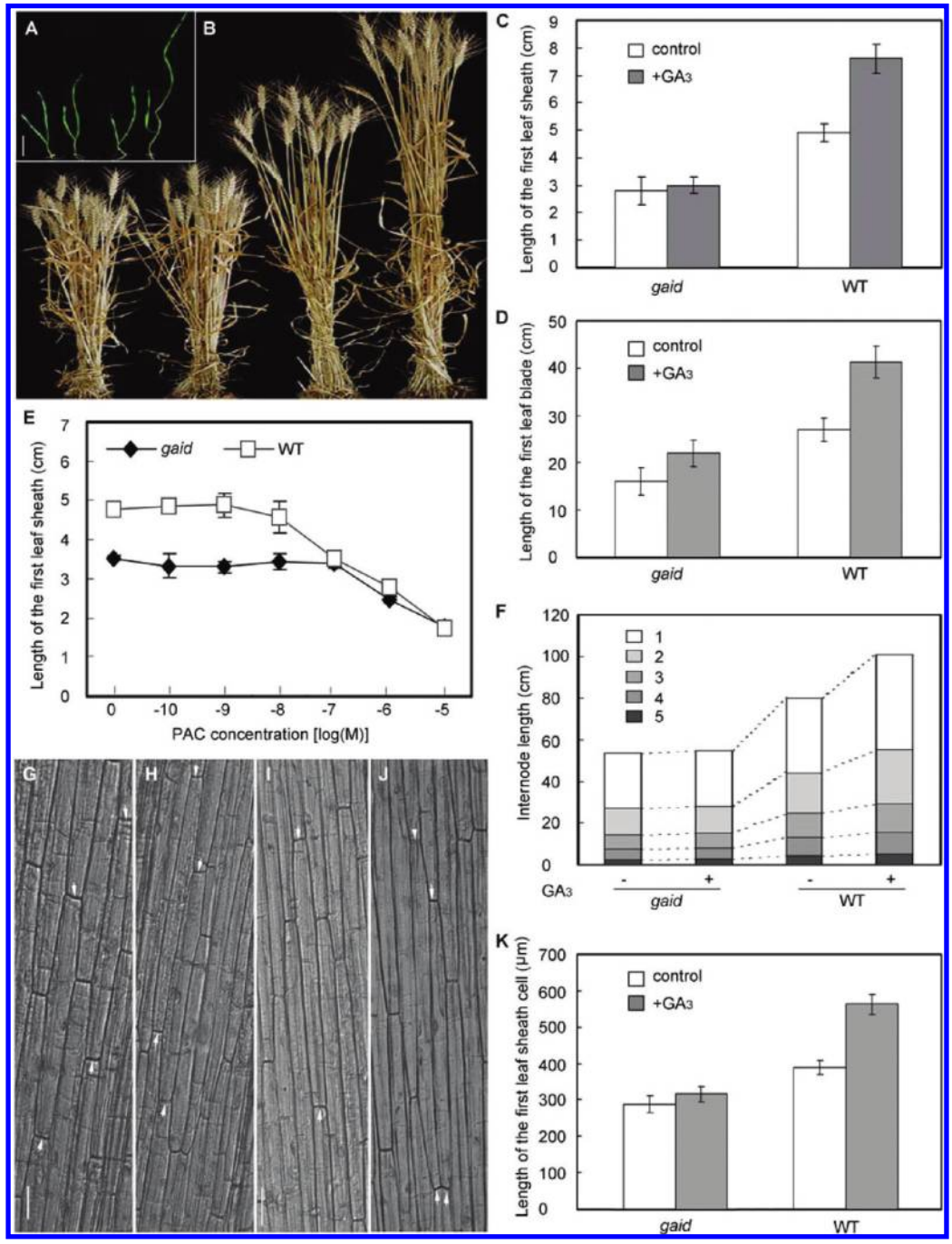

Figure 1. Phenotypic analysis of *gaid* mutant. (A) Plant height of *gaid* mutant treated with 10^{-4} M GA_3 in the seedling stage. From left to right: *gaid* mutant, *gaid* mutant treated with 10^{-4} M GA_3, the wild type and the wild type treated with 10^{-4} M GA_3. Bar: 5 cm. (B) Plant height of *gaid* mutant in the mature stage. From left to right: *gaid* mutant, *gaid* mutant treated with 10^{-4} M GA_3, the wild type and the wild type treated with 10^{-4} M GA_3. (C) Effects of GA_3 (10^{-4} M) on the first leaf sheath of *gaid* mutant and the wild type in the seedling stage. Results are means ± SE (D) Length of the first leaf blade of *gaid* mutant and the wild type with (+) or without (-) GA_3 in the seedling stage. Results are means ± SE (E) Internode length of *gaid* mutant and the wild type with (+) or without (-) GA_3. Data are mean internodes length of 30 plants. (F) Effect of paclobutrazol (PAC) on the growth of *gaid* mutant and the wild type. Results are means ± SE (G) Epidermal cells of the first leaf sheath of *gaid* mutant were observed under a differential interference contrast microscope. Bar: 50 μm. Arrowheads indicate the outline of the epidermal cell. (H) Epidermal cells of the first leaf sheath of *gaid* mutant treated with 10^{-4} M GA_3. (I) Epidermal cells of the first leaf sheath of the wild type. (J) Epidermal cells of the first leaf sheath of the wild type treated with 10^{-4} M GA_3. (K) Length of epidermal cells of the first leaf sheath. Results are means ± SE.

platform shaker). The enzyme solution turned green, indicated released protoplasts, which were checked under a microscope.

2.10. Generation of TaCYP20-2-overexpressed Transgenic Wheat. *TaCYP20-2* was amplified for construction with oligonucleotides 5′-CGGGATCCATGGCGGCCGCGACCTCCT-3′ and 5′-CCGGTACCTCAGACCACTGGAAGCTCCCC-3′ used as primers. The PCR fragment was cloned into the pUN1301 vector which carried a *β-glucuronidase* (*GUS*) gene as a marker. The *TaCYP20-2* gene was driven by the ubiquitin promoter. This construct was verified by sequencing and transformed into the

Table 1. Heterosis of Plant Height over the Parents[a]

male parent (♂)	height of male parent (cm)	height of F_1 (cm)	reducing effect (%)
ND3214	80 ± 1.5	70 ± 1.4	12.5%
ND99−5009	105 ± 0.8	72 ± 1.4	31.4%
Jing411	90 ± 1.4	75 ± 1.3	16.7%
BAU3338	55 ± 1.4	60 ± 1.0	−9.1%
gaid	60 ± 1.1	60 ± 1.1	

[a] *gaid* mutant was used as female parent. Beijing local varieties of winter wheat DN3214, ND99-5009, Jing411 and BAU3338 were used as male parents. ND means Nong Da. Results are presented as means ± SE.

Agrobacterium tumefaciens EHA105. The Agrobacterium-mediated transformation method for wheat was used as described by Supartana et al.[37]

3. Results

3.1. Genetic Effects of *gaid* Mutant on the Height of Wheat Varieties. A wheat mutant with dwarfism was screened from a natural population of variety wheat, Jingdong No.1. After 5 generations of selection, we established a wheat line with a dwarf phenotype during all growth stages from seedling to maturation as compared with the wild-type (Figure 1A−D,F). Leaves, leaf sheathes and stem in *gaid* were shorter than that in the wild type. The height-reduced percentage of *gaid* mutant was up to approximately 25% of the wild type from the seedling stage to heading. Numbers of the reduced percentage were quite close among leaves, leaf sheathes, and stem. To explore the genetic characters of *gaid*, the fifth generation plant as a female parent was crossed with the local varieties ND3214, ND99−5009, Jing411, as well as BAU3338, a dwarf mutant, as a male parent. The results showed a clear phenotype in height in progenies (Table 1). The height of most F_1 hybrid progenies of *gaid* mutant was lower than that of the local varieties (ND3214, ND99−5009, Jing411) and was 60−75 cm. In contrast, the height of the F_1 hybrid progenies of *gaid* and BAU3338 was higher than that of the male parent BAU3338 but was identical to that of their female parent, *gaid*. The similar thousand-grain weight of the wild type (50−60 g) and *gaid* plants (55−65 g; data not shown) indicates that the yield of *gaid* mutant was not negatively influenced.

3.2. Physiological Effect of GA_3 on *gaid* Growth. To elucidate the molecular mechanism of *gaid*, we tested the response of *gaid* to exogenous GA_3 treatment. Fifteen-day-old seedling of wild-type wheat responded positively to GA_3 treatment in shoot elongation (Figure 1A,C), and the length of the first leaf sheath increased by 57.4% (from about 4.7 to 7.4 cm). In contrast, in *gaid*, the length of the first leaf sheath had no significant difference compared with those of the same treatment ($P > 0.05$; Figure 1A,C).

As known, from the vegetative to reproductive stage, wheat internode elongation occurs only at the shoot apical meristem with exogenous GA_3 treatment. Figure 1B and C shows that the application of GA_3 did not result in internode elongation in *gaid*. In contrast, in the wild type, all of the first 5 internodes were elongated with exogenous GA_3 treatment, and shoot height increased from 90 to 110 cm. These results suggested that *gaid* was insensitive to GA_3 treatment.

To determine whether the reduction of shoot elongation in *gaid* was caused by either decreased cell elongation or cell number, epidermal layers of the first leaf sheath (approximately 5-mm of apex segment) were examined under a differential interference contrast microscope. Under the normal condition, the length of epidermal cells in the first leaf sheath of the wild type (388.6 μm) was much greater

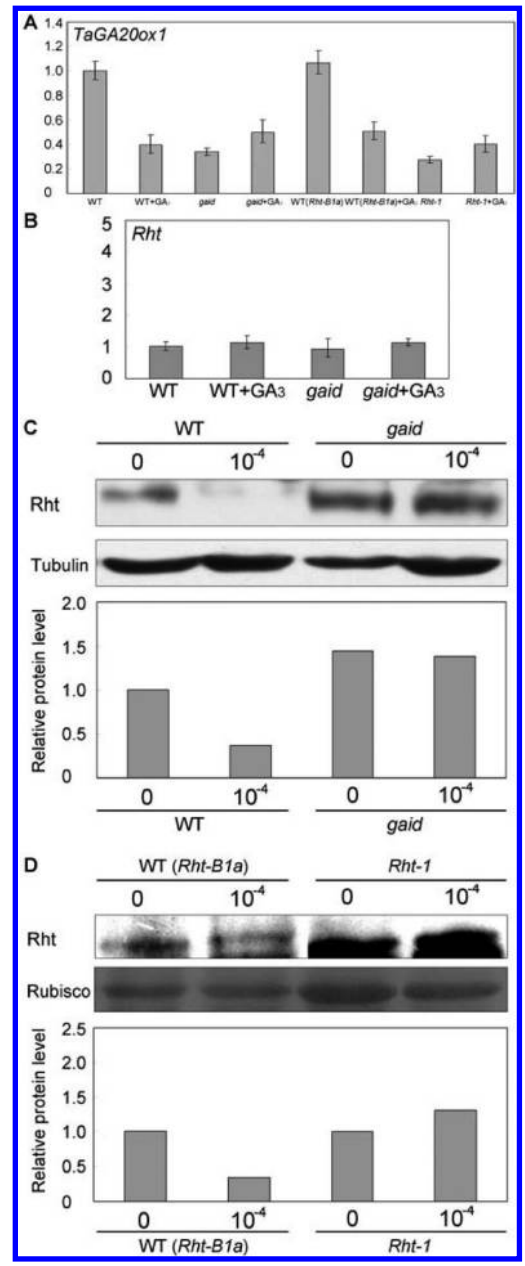

Figure 2. Expression analysis of *TaGA20ox1* and *Rht* in *gaid* and wild type (WT). (A) Quantitative real-time PCR analysis of *TaGA20ox1* gene transcripts in *gaid* mutants, the wild type, the wild type (*Rht-B1a*) and *Rht-1* mutant treated 10^{-4} M GA_3. (B) Quantitative real-time PCR analysis of *Rht* gene transcripts in *gaid* mutant and the wild type treated with 10^{-4} M GA_3. *Tubulin* gene was used as an internal control. Data represent means and SDs of the three replicates. (C) Immunoblotting of Rht involved 15 μg of protein of crude extract from the wild type and *gaid* treated with or without 10^{-4} M GA_3. Immunoblotting of α-tubulin protein was used as a loading control. The bottom is relative amount of Rht protein. The relative amount in wild type without GA_3 treatment was set as 1. (D) Immunoblotting of Rht involved 15 μg of protein of crude extract from the wild type (*Rht-B1a*) and *Rht-1* mutant treated with or without 10^{-4} M GA_3. Ponceau-S staining corresponding to Rubisco was used as a loading control. The bottom is relative amount of Rht protein. The relative amount in wild type without GA_3 treatment was set as 1.

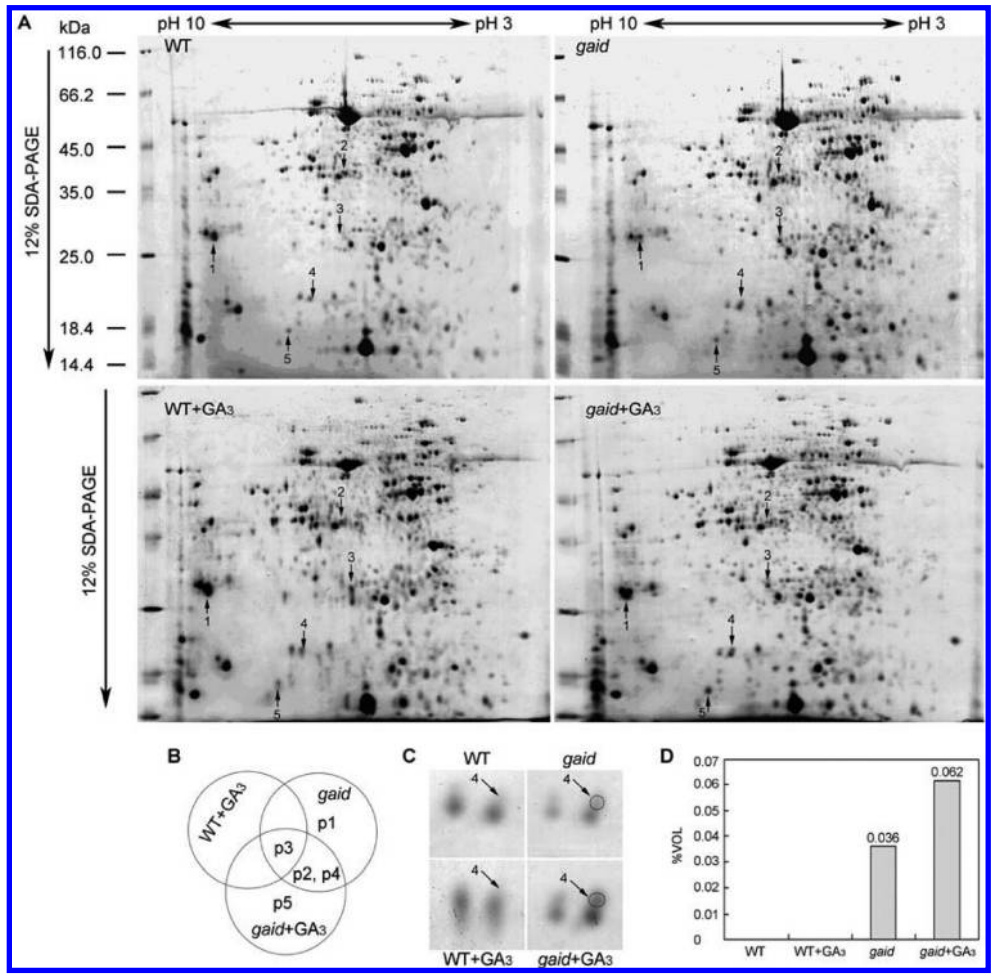

Figure 3. Representative 2-DE images of total aerial part proteins prepared from *gaid* mutant and the wild type (WT). (A) Aerial part proteins (600 μg) were separated on 24-cm IPG (pH 3−10) strips in the first dimension followed by 12% SDS-PAGE. (B) Venn diagram of protein spots regulated by GA_3 treatment, the *gaid* mutant, and the *gaid* mutant treated with GA_3. (C) Enlarged images of protein spot 4 on gels. (D) The gel images correspond to (C) as the %Vol shown.

than that of *gaid* (289 μm; Figure 1H,F,J). After GA_3 treatment with 100 μM for 24 h, the mean length of epidermal cells of the wild type was increased by 45%, to 562.3 μm (Figure 1I,J). But the effect of the GA_3 treatment on epidermal cells in *gaid* (316.4 μm; Figure 1G,J) did not reach a level with statistical significance ($P > 0.05$).

The *gaid* plants are more insensitive to PAC, a GA biosynthesis inhibitor, than the wild type. Dose−response results with PAC treatment (Figure 1E) showed that the first leaf sheath length of the wild type was inhibited at 10^{-8} M. At 10^{-7} M of PAC, the wild type was dwarfed similar to *gaid*. In contrast, the length of the first leaf sheath in *gaid* did not change with PAC treatment up to 10^{-7} M. At a higher concentration of PAC (>10^{-7} M), the first leaf sheath length in both *gaid* mutant and the wild type was reduced to the same level.

3.3. Expression Patterns of *TaGA20ox1* and Rht in *gaid*. As known, mutants with impaired response to GAs have always elevated GA biosynthesis genes expression and reduced DELLA protein turnover.[38] To investigate whether transcriptional pattern on genes in GA biosynthesis was changed in *gaid*, we monitored the transcript level of *TaGA20ox1* gene. The results revealed that treatment of the wild type with GA_3 for 3 h induced a drastic reduction in mRNA level of *TaGA20ox1* (Figure 2A). However, the transcript level of *TaGA20ox1* in *gaid* increased slightly after GA_3 treatment. The expression pattern response of *TaGA20ox1* in *Rht-1* wheat mutant was lightly elevated with GA_3 treatment (Figure 2A), which was similar to that in the *gaid* mutant. In *Rht-B1a* wheat allele as the wild type, contrarily, a significant decrease transcript level of *TaGA20ox1* appeared after GA_3 treatment.

The gain-of-function mutation of *Rht* can suppress the effects of GA in wheat with phenotypes of dwarfism and GA-insensitivity.[2] The analysis of the *Rht-D1a* gene in the genome of *gaid* mutant indicated that the open reading frame sequences was the same as wild type (data not shown). Real-time PCR results showed that mRNA level of *Rht-D1a* was similar between *gaid* and wild-type plants whether with GA_3 treatment or not (Figure 2B). The Rht protein expression pattern on immunoblotting assay (Figure 2C) showed that its level decreased after GA_3 treatment in the wild type. In *gaid* mutant, on the contrary, any response of the Rht protein level to GA_3 on degradation was not detected. As a typical DELLA mutant response, the expression pattern response of Rht in *Rht-1* wheat mutant was not decrease after the treatment of GA_3 (Figure 2D). Contrarily, Rht protein decreased significantly with GA_3 treatment in its wild type plants. It suggested that the degradation of Rht induced by GA was suppressed in *gaid* mutant.

3.4. Global Proteomic Analysis of *gaid* and Identification of the Differentially Expressed Proteins. A comparative proteomic approach was used to explore the mechanism of dwarfism in *gaid*. Total aerial part proteins extracted from *gaid*

Table 2. Identification of Differentially Induced Proteins in *gaid* Mutant

spot no.	protein name	accession number	MOWSE score	organism	matched peptides	M_r	p*I*	sequence coverage (%)
1	Predicted protein	XP_001753354	43	Physcomitre -lla patens	1	18.8	9.4	46
2	ATP synthase CF1 alpha chain	NP_039282	66	Marchantia polymorpha	9	55.3	5.3	26
3	hypothetical protein	AP004260h	67	*Oryza sativa*	6	16.9	9.2	47
4	Peptidylproyl isomerase	ABO37960	117	*Triticum aestivum*	5	26.0	9.4	17
5	Cyclophilin A-1	AAK49426	129	*Triticum aestivum*	5	18.7	8.5	22

and the wild type were separated by 2-DE. The representative 2-DE leaf protein maps are shown in Figure 3A. ImageMaster analysis of at least three independent gels revealed about 500 protein spots reproducibly resolved on Coomassie-stained gels over a combined pH of 3−10 and molecular weight (MW) 6−120 kDa in *gaid* or wild type. Although more than 99% of the protein spots remained with consistent expression levels in *gaid* and the wild type, 5 protein spots (name as spot 1 to spot 5; Figure 3A) were reproducibly detected as changed in their protein levels. Figure 3B showed the Venn diagram analysis of these differentially expressed spots at various samples. Both spot 1 and spot 2 were down-regulated, and contrarily, spot 3 and spot 4 were up-regulated in *gaid* as compared with the wild type. There was no changed pattern in spot 5 in the mutant compared with the wild type. After GA_3 treatment, spot 5 was accumulated more in *gaid* than that in the wild type. Of note, spot 4 could still not be observed in the wild type under GA_3 treatment on Coomassie-stained gels. Moreover, in *gaid*, spot 4 was not significantly accumulated after the treatment (Figure 3C,D). The expression pattern of spot 4 in *gaid* was independent of GA_3 treatment.

Differentially expressed proteins were excised from the gels, in-gel digested by trypsin, and identified by a Q-TOF MS. The results showed that spot 1 and spot 3 were characterized as a predicted and a hypothetical protein respectively. Spot 2 was identified as ATP synthase CF1 alpha chain. Spot 4 and spot 5 were revealed corresponding to wheat cyclophilin family proteins. Spot 5 matched a cylophilin A-1 protein, and spot 4 corresponded to a cyclophilin-like protein (TaCYP20-2) (Table 2).

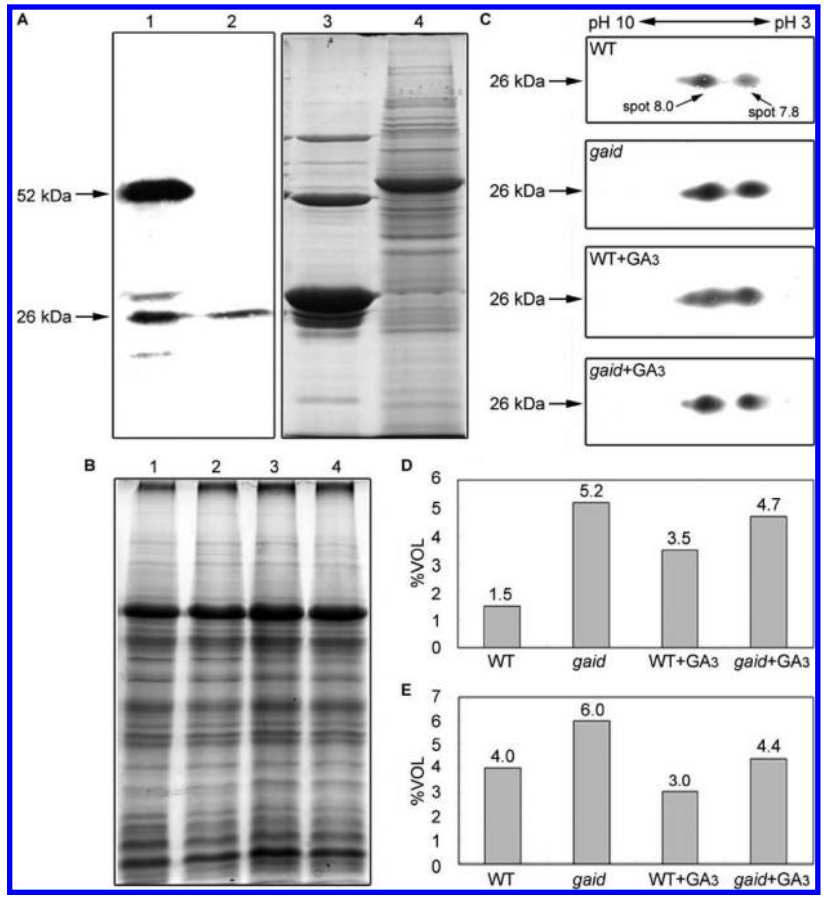

Figure 4. Immunoblot analysis of TaCYP20-2 expression in *gaid* mutant. (A) The specificity test of polyconal TaCYP20-2 antibody. Purification of GST-TaCYP20-2 recombinant protein (lane 1) and leaf protein extracted from wheat (lane 2) were separated by 12% SDS-PAGE and detected by polyclonal TaCYP20-2 antibody. Lane 3 and lane 4 were the Coomassie brilliant blue (CBB)-stained GST-TaCYP20-2 recombinant protein and whole leaf protein as a loading control. (B) Loading control of immunoblot analysis of TaCYP20-2 protein level (C) in the wild type (lane 1), *gaid* mutant (lane 2), the wild type treated with GA_3 (lane 3), and *gaid* mutant treated with GA_3 (lane 4). (C) Leaf protein (80 μg) of wild type, *gaid* mutant, the wild type treated with GA_3, and gaid mutant treated with GA_3 were separated by 2-DE and detected by polyconal TaCYP20-2 antibody. (D) %Vol of detected spot 7.8 by immunoblotting. (E) %Vol of detected spot 8.0 by immunoblotting.

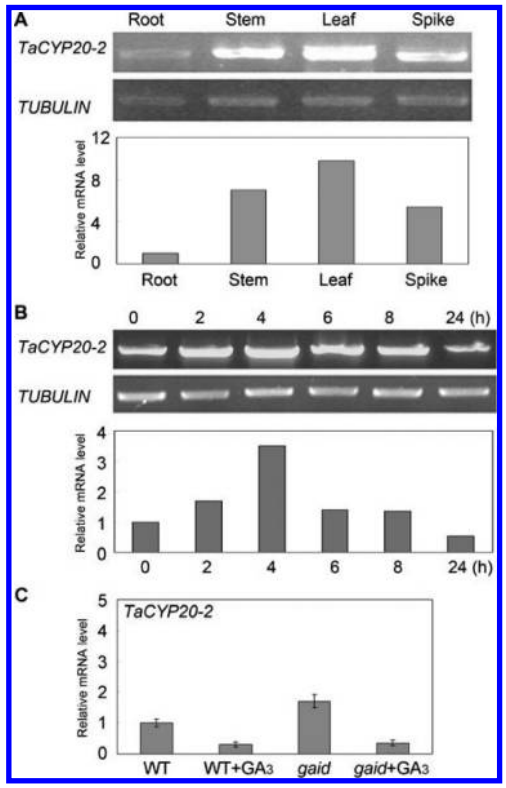

Figure 5. Expression pattern of *TaCYP20-2* in the wild type and *gaid* mutant wheat. (A) Semi-quantitative RT-PCR results showed *TaCYP20-2* expressed in roots, stems, leaves and spikes. (B) Semi-quantitative RT-PCR results showed expression of *TaCYP20-2* responding to GA_3 treatment. Bars represent relative amount of the normalized expression of *TaCYP20-2* in response to GA_3 treatment. (C) Quantitative real-time PCR analysis of *TaCYP20-2* gene transcripts in *gaid* mutants and the wild type treated with 10^{-4} M GA_3.

3.5. Confirmation of the Accumulation of TaCYP20-2 Protein in *gaid*. To confirm the results of 2-DE and MS, the protein level of TaCYP20-2 in *gaid* was monitored by immunoblotting. The specificity of the antibody raised against TaCYP20-2 was detected first. Theoretically, TaCYP20-2 is 25.9 kDa. Two stronger bands at 52 kDa and 26 kDa were recognized in the blot by the antibody in purified the GST-tagged recombinant TaCYP20-2 protein (Figure 4A). In the whole protein extract of the wild-type wheat, the immunoblotting showed the antibody with specificity to a 26-kDa protein, which was consistent with TaCYP20-2 (Figure 4A).

The protein extracts from the aerial part of the wild type and *gaid*, as well as the treated ones, were separated by 2-DE with IEF (pH 3−10; 7 cm) for the first dimension and 12% SDS-PAGE for the second dimension. Then the four gels were blotted and detected by the antibody raised against TaCYP20-2. The immunoblotting with 2-DE gels (Figure 4C) showed two TaCYP20-2 isoforms with different p*I* values (8.0 and 7.8). Since the observed p*I* values were different from the theoretical one (p*I* 9.4), we assumed that the discrepancy between its observed p*I* values and theoretical one resulted from an acidic shift, and the two protein spots (spot 8.0 and spot 7.8) represented the different post-translational modification of TaCYP20-2. The observed p*I* value of spot 4 was also 7.8. The kinetics of protein-abundance change of spot 7.8 determined by immunoblot (Figure 4C,D) was very similar to that measured by 2-DE (Figure 3C,D). Spot 7.8 was up-regulated in *gaid* compared with that in the wild type (Figure 4C,D). In *gaid*, the protein level of spot 8.0 was also slightly higher than that in the wild type (Figure 4C,E). These results confirmed TaCYP20-2 was accumulated in *gaid* compared with that in the wild type.

3.6. Expression of TaCYP20-2 in Wheat and its Response to GA_3. The *TaCYP20-2* gene contains an open reading frame of 245 amino acids, with molecular mass 25.9 kDa and p*I* 9.40. TaCYP20-2 protein is constituted by only a single cyclophilin_ABH domain, which is the core domain of the cyclophilin family.[39,40] To explore the relation between TaCYP20-2 and other single-domain cyclophilins, a sequence-based phylogenetic tree was constructed (Supplementary Figure 1A in Supporting Information). The polygenetic tree consists of three major groups. TaCYP20-2 and TaCYP20-c are different copies of the same gene in hexaploid wheat. Rice protein NP_001054392 is an ortholog of TaCYP20-2, which showed the highest identity (82%) with TaCYP20-2 protein. The *Arabidopsis* ortholog with the highest similarity (67%) is AtCYP20-2. Alignment analysis showed that TaCYP20-2 gene shared higher sequence similarity with single-domain cyclophilins from rice, *Arabidopsis*, maize, tomato, bean and human (Supplementary Figure 1B in Supporting Information).

The mRNA level of *TaCYP20-2* in various wheat tissues was detected by semiquantitative RT-PCR (Figure 5A). The result indicated that the transcript of *TaCYP20-2* was constitutive of expression in various tissues. Preponderant expression appeared in young leaves. The transcriptional time course in response to GA_3 in the wild type showed that the *TaCYP20-2* mRNA level increased rapidly within 4 h under GA_3 treatment (Figure 5B). Subsequently, the mRNA level began to decline up to 24-h treatment. These results indicated that the mRNA

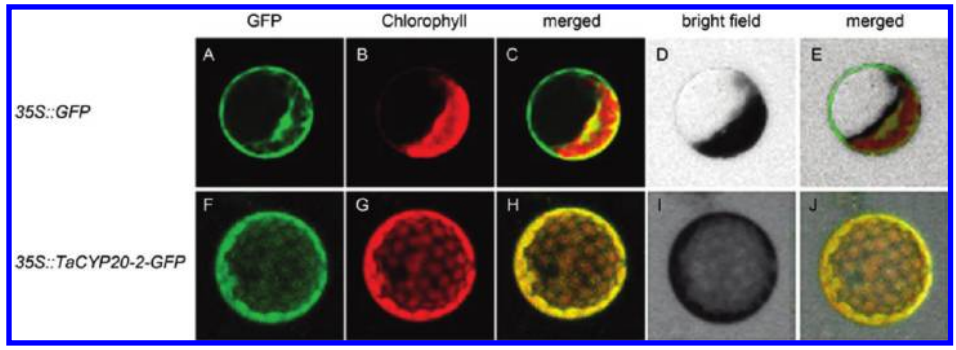

Figure 6. Subcellular localization of TaCYP20-2:green fluorescent protein (TaCYP20-2:GFP). (A)−(E) Protoplast transformed with empty pBI221 vector used as a control. (F)−(J) Protoplast was isolated from *35S::TaCYP20-2:GFP* transgenic Arabidopsis. Green and red images are GFP and chlorophyll autonomous fluorescent signals respectively. Corresponding bright-field images [(D) and (I)]. Bar: 20 μm.

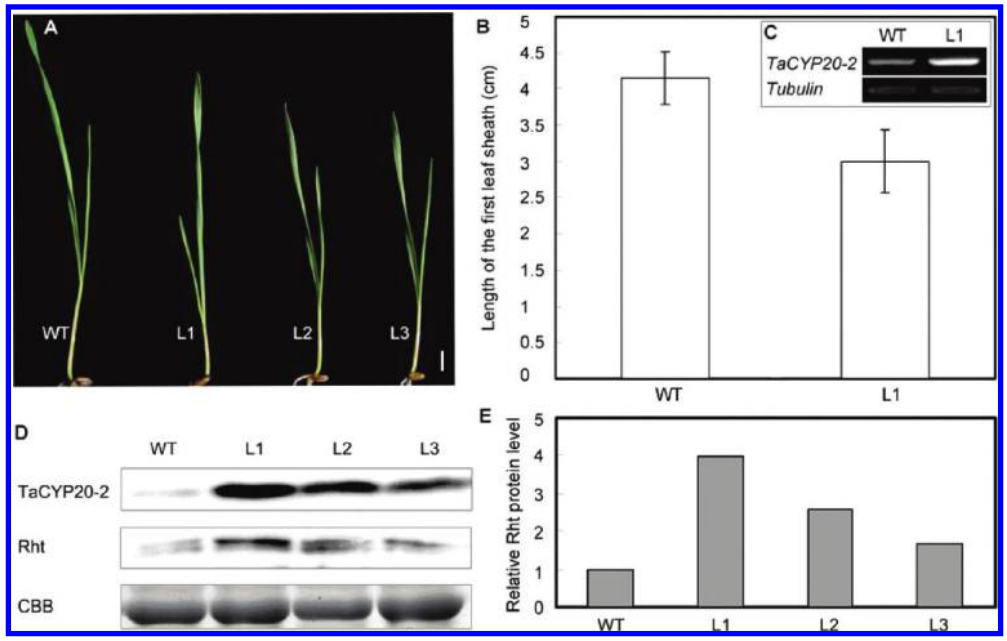

Figure 7. Phenotype of *TaCYP20-2* constitutive expression plants. (A) Plant height in the seedling stage. From left to right: the wild type and *ubiquitin::TaCYP20-2* L1-1, L1-2 and L1-3. Bar: 1 cm. (B) Comparison of the first leaf sheath of the wild type and *ubiquitin::TaCYP20-2*. Results are means ± SE. (C) Level of *TaCYP20-2* mRNA in the wild type and transgenic wheat. *Tubulin* was used as a control. (D) Immunoblotting of TaCYP20-2 and RHT expression in TaCYP20-2-overexpressed transgenic wheat. L1-3: three independent transgenic lines. The Coomassie brilliant blue-stained Rubisco protein was used as a loading control (CBB). (E) Relative amount of Rht protein in the *TaCYP20-2* overexpression transgenic wheat lines based on immunoblotting in D. Relative amount in wild type was set as 1.

level of *TaCYP20-2* was induced by GA_3, which is consistent with the data on protein level described above (Figure 4C,D). Real-time PCR analysis revealed that mRNA level of *TaCYP20-2* in *gaid* mutant wheat was slightly higher than that in the wild type (Figure 5C). After GA_3 treatment, the *TaCYP20-2* mRNA level declined to the similar level between the wild type and *gaid* mutant.

3.7. Subcellular Localization of TaCYP20-2:GFP Fusion Protein. To examine its subcellular localization, *TaCYP20-2* from wheat was fused with *GFP* reporter gene under the control of the CaMV 35S promoter and transformed into *Arabidopsis*. Protoplasts were isolated from *35S::TaCYP20-2-GFP* transgenic *Arabidopsis* leaves. Fluorescence analysis revealed that TaCYP20-2-GFP signals were mainly spots and on the edge of protoplasts, whereas the GFP signals alone appeared in the whole protoplasts (Figure 6). Moreover, GFP signals could overlap with red fluorescence signals of chloroplasts. Thus, *TaCYP20-2* is specifically localized in the chloroplast and cell plasma membrane.

3.8. Phenotype of TaCYP20-2-Overexpressed Transgenic Wheat. A construct of *TaCYP20-2* driven by the ubiquitin promoter was transformed into wheat plants to create three T_0 generation lines of transgenic plants. The transformation lines were screened by hygromycin as well as genomic PCR (data not shown). *TaCYP20-2* transgenic wheat (Figure 7) was confirmed by semiquantitative RT-PCR. *TaCYP20-2* was detected in the wild-type plants, but the transgenic line showed a much higher expression level (Figure 7C). The immunoblotting result showed the protein level of TaCYP20-2 was increased significantly in transgenic lines, such as L1, L2 and L3, which agrees with the results of RT-PCR (Figure 7D). The changed protein expression pattern of Rht was detected by immunoblotting in *TaCYP20-2* overexpression transgenic wheat lines. The result indicated Rht protein accumulated higher in all three *TaCYP20-2* transgenic lines than that in the wild type (Figure 7D and E).

Table 3. Height (cm) of the Wild-Type and T_1 Transgenic Wheat after Heading[a]

Wild type	50.12 ± 5.47
Transgenic Line1	39.34 ± 2.66

[a] Results are presented as means ± SE.

To examine the possible phenotypes of transgenic wheat, T_0 and T_1 generations of *TaCYP20-2*-overexpressed wheat, as well as the wild-type plants, were grown in the field after vernalization for 30 days. Compared with the wild-type plants, the transgenic wheat showed a clear dwarf phenotype during all growth stages from seedling (Figure 7A) to maturation (Table 3), which was similar to the dwarf phenotype of *gaid*. The length of the first leaf sheath of *TaCYP20-2*-overexpressed wheat was less than that of the wild type at the seedling stage (Figure 7B). After heading, the height of *TaCYP20-2*-overexpressed plants reached approximately 75% of that of the wild type (Table 3). The difference in height between the wild type and *TaCYP20-2*-overexpressed wheat was statistically significant ($P < 0.05$).

4. Discussion

4.1. The *gaid* Dwarf Mutant is a New Variety for "Green Revolution" Breeding. In grain crops, dwarfism of wheat and rice cultivars is a major factor for the success of the "Green Revolution". For instance, *sd1* semidwarf rice and *Rht* semidwarf wheat have been widely utilized in crop improvement for higher grain yield. In this study, we characterized a novel dwarf wheat mutant, *gaid*. The semidominant dwarf phenotype of *gaid* could be stably inherited. Except for the dwarf mutant BAU3338, the local cultivars showed reduced height after hybrid with *gaid* (Table 1). The progenies with reduced height retained the same seed weight as that of their parents. Therefore, *gaid* could be a good variety candidate for "Green Revolution"

because of its moderate dwarfism in relation to stem growth and panicle development.

The dwarf phenotype of *gaid* with treatment of GA_3 can not be rescued (Figure 1). Plants of *gaid* responded less to GA_3 than wild type in terms of the first leaf sheath elongation. Moreover, *gaid* mutant plants responded to PAC with a concentration 10 times higher than the wild type did, which indicates that dwarfism of *gaid* mutant is independent of endogenous GA level at normal physiological status. The wheat *Rht* mutant (*Rht-B1b* and *Rht-D1b*) also showed only a slight growth response to GA_3, even at high concentration.[2] The length of Leaf sheath epidermal cells in *gaid* is much shorter than the wild type (Figure 1). It indicates that the dwarfism of *gaid* resulted from reduced cell elongation. The *Rht-B1b* and *Rht-D1b* GA-insensitive dwarfing genes are able to decrease cell wall extensibility to reduce epidermal cell length.[41] Therefore, it is possible that the shortened leaf sheath cell length in *gaid* resulted from up-regulated *Rht* gene expression. Changed expression of GA biosynthesis genes by GAs induction has been described in several GA-insensitive mutants.[42] GA 20-oxidase is a primary target for feedback regulation. As known, the gain-of-function mutations in the repressors or loss-of-function mutations in the positive components of the GA response pathway often lead to an up-regulation of *GA20ox* gene expression.[42] For example, *GA20ox* gene mRNA level decreased in the wild type *Arabidopsis* after GA_4 treatment, while the level increased slightly in the *gai* mutant.[11,38] The changed patterns of *TaGA20ox1* transcript level under GA_3 treatment in *gaid* and *Rht-1* (Figure 2) are comparable to above phenomenon of *Arabidopsis*. Treating the plants with GA_3 caused *TaGA20ox1* mRNA level declining in the wild type. In contrast, the level increased slightly in *gaid* and *Rht-1*. However, our data on *GA20ox1* expression patterns showed that the basal expression level of *TaGA20ox1* either in *gaid* or *Rht1* mutant was lower that in their relative wild type plants, respectively. It is possible that others GA oxidases, such as GA20ox-2, GA2ox and GA3ox, may respond in the mutants. At a minimum, there are two GA 20-oxidase genes (*GA20ox-1* and *GA20ox-2*) and *SD1* corresponded to *GA20ox-2* in the rice genome. *GA20ox2* is highly expressed in leaves and flowers, whereas *GA20ox1* is preferentially expressed in the flowers.[43] Mutants with impaired responses to GA have always elevated GA biosynthesis genes expression and reduced DELLA protein turnover.[38] The DELLA protein Rht was accumulated in *gaid* mutant similar to *Rht-1* wheat mutant (Figure 2). These phenotypes of *gaid* suggest that it is due to mutations in a gene participating in a GA signaling pathway rather than a GA biosynthesis pathway. The sequence of the *Rht* gene was conservative in genome of the *gaid* mutant (data not shown). These evidence as well as the physiological ones on the response to GA_3 suggest that *gaid* is a new semidwarf wheat mutant in the GA signaling pathway through a different mechanism from that of published mutants, including *Rht* and *Sln*.

4.2. Accumulation of TaCYP20-2 Causes Dwarf in Wheat. In this work, comparative proteomics as a powerful quantitative experimental strategy is first applied for investigating wheat mutant. Using this approach, we identified some regulated proteins as candidates for proteins with important roles in *gaid*. Most convincingly, we found the protein level of TaCYP20-2 was accumulated in *gaid* (Figure 3). Immunoblotting provided further evidence similar to this result of 2-DE (Figure 4). On the basis of Real-time PCR results (Figure 5), we considered that the higher transcript level of *TaCYP20-2* gene resulted in the accumulation of TaCYP20-2 protein in *gaid*. Because wheat genome is a hexaploid, most allele genes are of functional redundancy. Almost all of the wheat mutants are resulted from dominant gain-of-function mutations. Accordingly, we propose a hypothesis that the accumulation of TaCYP20-2 should be associated with the dwarf phenotype in *gaid*.

TaCYP20-2 possesses all of the key structural features of the cyclophilin family (Supplementary Figure 1 in the Supporting Information). In human cyclophilin A, Trp-121 was identified as a residue required for CsA binding but not participated in PPIase enzymatic activity by mutagenesis studies.[44,45] Moreover, mutations in Arg-55, Phe-60 and His-126 result in PPIase enzymatic activity reduced to 1% of original human cyclophilin A activity.[45] Therefore, corresponding conservative amino acid residues in TaCYP20-2 may play vital roles. TaCYP20-2 was predicted to be targeted to the chloroplast and had no transmembrane region by the neural-network-based targeting prediction program TargetP (data not shown). However, subcellular localization analysis results indicated that the TaCYP20-2-GFP fusion protein accumulated mainly in the chloroplast and cell plasma membrane (Figure 6). Expression-pattern analysis showed TaCYP20-2 is in various tissues of wheat (Figure 5). The results suggest that TaCYP20-2 protein was not only restricted to the photosynthetic tissue but also attached to the cell membrane. On the basis of this evidence, it is possible that TaCYP20-2 plays a role during signaling transduction.

Previous reports have indicated that cyclophilins have a great influence on the sensing and signaling pathways of plant hormones. LeCYP1, a tomato type-A cyclophilin highly homologous to human cyclophilin A, is induced by auxin treatment and essential for morphogenesis of lateral root primordial.[46] According to that, FKBP42 is present in the plasma membrane and interacts with the multidrug resistance/P-glycoprotein (PGP); FKBP42 is proven to play a positive regulatory role in PGP-mediated export of auxin.[47] Studies of the *Arabidopsis pas1* mutant indicated that *FKBP70* was involved in cell division through cytokinin signaling pathway.[28] Accumulation of the heat-stress protein FKBP77 in wheat also has a negative effect on plant development, especially causing dwarfism.[48] These evidence raise the possibility that the accumulation of TaCYP20-2 may cause dwarfism of *gaid* through GA signaling pathway. Consistent with *gaid* mutant wheat, *TaCYP20-2*-overexpressing transgenic wheat showed a 25% shorter stem than the wild type from seedling to mature stage (Figure 7 and Table 3), which indicates that *TaCYP20-2*-overexpressed transgenic wheat displays a dwarf phenotype. These findings indicate the accumulation of TaCYP20-2 would induce dwarfism in wheat.

4.3. Degradation Suppression of DELLA Protein Mediated by the Accumulation of Cyclophilin is Involved in *gaid* Mutant. The *gaid* mutation resulted in the semidominant dwarf blocking of the GA signaling pathway, a phenotype analogous to that of the gain-of-function mutation of *Rht* in wheat[2] and *GAI* in *Arabidopsis*.[11] The transcript levels of *Rht-D1a* did not change in *gaid* seedlings with or without GA_3 treatment, similar to that in wild-type (Figure 2B). *Rht-D1a* gene in *gaid* genome showed no mutation at DNA sequence as compared with the wild type. There is a great probability that the accumulation of Rht protein leads to *gaid* mutant. In wild-type plants, bioactive GAs can depress the action of negatively acting components such as GAI/SLR/SLN/RHT and regulate the degradation of these repressor proteins during seed germina-

tion and shoot growth.[19] Rht protein in *gaid* did not respond to GA_3 treatment, whereas it declined significantly after GA_3 treatment in the wild-type plants (Figure 2C). Remarkable up-regulation of Rht protein level had been observed in the transgenic wheat lines (Figure 7D and E). These results strongly support the idea that there is a positive correlation between the protein levels of Rht and TaCYP20-2. The protein level of TaCYP20-2 in *gaid* mutant is about three times higher than that in the wild type. The difference of Rht protein between *gaid* mutant and the wild type without GA_3 treatment is less evident in the immunoblotting analysis. However, in the transgenic wheat, TaCYP20-2 level is dozens of times higher than that in the wild type. Meanwhile, the protein change trends of TaCYP20-2 and Rht in different transgenic wheat lines are consistent. It suggests that Rht degradation may be suppressed in *gaid* mutant. It becomes clear that the dwarfism of *gaid* did not result from the mutation in *Rht-D1a* gene, but, rather, the accumulation of Rht protein. Taken together, the *TaCYP20-2*-overexpressed transgenic wheat showed a higher level of Rht protein and reduced plant height. These properties are also characteristics of *gaid* mutant, indicating that *gaid* mutant is caused by the accumulation of TaCYP20-2 protein. On the basis of the evidence that the transcription of *TaCYP20-2* was increased in the *gaid* mutant (Figure 5C) and there was not any difference on the gene sequences between the mutant and wild type (data not shown), it is possible that there is an unknown element to stimulate the *TaCYP20-2* transcription on genome resulting in the dwarf mutant.

The research on the cyclophilin-like domain of Ran-binding protein-2 (RanBP2) in human cells revealed that it selectively promoted the accumulation of properly folded targets of the ubiquitin-proteasome system for degradation.[49] It is well-known that DELLA proteins are targets of the ubiquitin-proteasome system.[17,18] The expression level of Rht increased in the transgenic wheat compared with the wild type (Figure 7). Combined with previous results that the degradation of Rht protein was repressed in *gaid* (Figure 2), it is reasonable to deduce that the accumulation of TaCYP20-2 causes an increase in Rht protein abundance and leads to dwarfism phenotype of *gaid* according to the gain-of-function mutation of *Rht* in wheat. A cyclophilin protein was identified as a peptidyl-prolyl cis−trans isomerase (PPIase) in spinach. It catalyzes the key step for protein folding, which was shown in the thylakoid lumen.[23] The selective effect of cyclophilin protein on the ubiquitin-proteasome system is a synergy with proteasome inhibitors or factors to suppress activity of the 26S proteasome. The factor(s) may be necessary to mediate the post-translational modification and to inhibit its recognition by a pool of ubiquitinated substrates.[49] Like that in human cells, it is possible the cyclophilin-like protein selectively modulates the activity of the ubiquitin-proteasome system through its interaction with inhibitor(s) to regulate the turnover of properly folded proteins which are essential for plant development. Such a scenario might explain, at least in part, the intriguing roles that TaCYP20-2 appears to play as a negative regulator in GA signaling pathway through modulating DELLA protein abundance. GAID/CYP20-2 as a PPIase may be involved in protein modulation and/or protein folding to impact proteasome system. It should be substantiated with further experimental evidence in the future.

5. Conclusions

This report has characterized a novel dwarf wheat mutant, *gaid*, which is a very useful genetic source for conventional hybrid breeding and deep understanding of the mechanism of GA signaling pathway. Furthermore, we first provide comparative proteomic and immunoblotting evidence to reveal TaCYP20-2 enriched in *gaid*. This, combined with the discovery of *TaCYP20-2*-overexpressed transgenic wheat exhibiting a dwarf feature similar to that of *gaid* mutant wheat, suggested that the accumulation of TaCYP20-2 is involved in the regulation mechanism of dwarfism in the *gaid* mutant. As known, the cell extension for growth is controlled by the signaling pathway of GAs-mediated DELLA protein degradation. Our data on the relation between cyclophilin and DELLA protein indicates that TaCYP20-2 is a new negative regulator in the GA signaling transduction pathway of DELLA protein degradation for cell extension in nature case. This report provides beneficial information for molecular breeding leading to "Green Revolution" of agricultural crops.

Acknowledgment. We thank Dr. Zhiyong Wang (Department of Plant Biology, Carnegie Institution for Science, U.S.A.) and Dr. Xiangdong Fu (Institute of Genetics and Development biology, CAS) for their useful comments on the project and the manuscript and Dr. Frank Gubler (Commonwealth Scientific and Industrial Research Organization, Canberra, Australia) for his generous gift of antibodies against SLN1. This work was supported by the National Science Foundation of China for Innovative Research Groups (grant no. 30821007) and the Innovation Project of CAS.

Supporting Information Available: Supplementary Figure showing phylogenetic tree of cyclophilin proteins from different organisms (A), and alignment of the amino acid sequence for TaCYP20-2 and sequences encoded by related genes of wheat, rice, *Arabidopsis*, maize, tomato, fava bean and human (B). This material is available free of charge via the Internet at http://pubs.acs.org.

References

(1) Conway, G.; Toenniessen, G. Feeding the world in the twenty-first century. *Nature* **1999**, *402*, C55–58.
(2) Peng, J.; Richards, D. E.; Hartley, N. M.; Murphy, G. P.; Devos, K. M.; Flintham, J. E.; Beales, J.; Fish, L. J.; Worland, A. J.; Pelica, F.; Sudhakar, D.; Christou, P.; Snape, J. W.; Gale, M. D.; Harberd, N. P. 'Green revolution' genes encode mutant gibberellin response modulators. *Nature* **1999**, *400*, 256–261.
(3) Ellis, H.; Spielmeyer, W.; Gale, R.; Rebetzke, J.; Richards, A. Perfect" markers for the Rht-B1b and Rht-D1b dwarfing genes in wheat. *Theor. Appl. Genet.* **2002**, *105*, 1038–1042.
(4) Fujioka, S.; Yamane, H.; Spray, C. R.; Katsumi, M.; Phinney, B. O.; Gaskin, P.; Macmillan, J.; Takahashi, N. The dominant non-gibberellin-responding dwarf mutant (D8) of maize accumulates native gibberellins. *Proc. Natl. Acad. Sci. U.S.A.* **1988**, *85*, 9031–9035.
(5) Ho, T. H.; Nolan, R. C.; Shute, D. E. Characterization of a Gibberellin-Insensitive Dwarf Wheat, D6899: EVIDENCE FOR A REGULATORY STEP COMMON TO MANY DIVERSE RESPONSES TO GIBBERELLINS. *Plant Physiol.* **1981**, *67*, 1026–1031.
(6) Ikeda, A.; Ueguchi-Tanaka, M.; Sonoda, Y.; Kitano, H.; Koshioka, M.; Futsuhara, Y.; Matsuoka, M.; Yamaguchi, J. slender rice, a constitutive gibberellin response mutant, is caused by a null mutation of the SLR1 gene, an ortholog of the height-regulating gene GAI/RGA/RHT/D8. *Plant Cell* **2001**, *13*, 999–1010.
(7) Peng, J.; Richards, D. E.; Moritz, T.; Cano-Delgado, A.; Harberd, N. P. Extragenic suppressors of the Arabidopsis gai mutation alter the dose-response relationship of diverse gibberellin responses. *Plant Physiol.* **1999**, *119*, 1199–1208.

(8) Spielmeyer, W.; Ellis, M. H.; Chandler, P. M. Semidwarf (sd-1), "green revolution" rice, contains a defective gibberellin 20-oxidase gene. *Proc. Natl. Acad. Sci. U.S.A.* **2002**, *99*, 9043–9048.
(9) Sun, T. P.; Kamiya, Y. The Arabidopsis GA1 locus encodes the cyclase ent-kaurene synthetase A of gibberellin biosynthesis. *Plant Cell* **1994**, *6*, 1509–1518.
(10) Asano, K.; Hirano, K.; Ueguchi-Tanaka, M.; Angeles-Shim, R. B.; Komura, T.; Satoh, H.; Kitano, H.; Matsuoka, M.; Ashikari, M. Isolation and characterization of dominant dwarf mutants, Slr1-d, in rice. *Mol. Genet. Genomics* **2009**, *281*, 223–231.
(11) Peng, J.; Carol, P.; Richards, D. E.; King, K. E.; Cowling, R. J.; Murphy, G. P.; Harberd, N. P. The Arabidopsis GAI gene defines a signaling pathway that negatively regulates gibberellin responses. *Genes Dev.* **1997**, *11*, 3194–3205.
(12) Chandler, P. M.; Marion-Poll, A.; Ellis, M.; Gubler, F. Mutants at the Slender1 locus of barley cv Himalaya. Molecular and physiological characterization. *Plant Physiol.* **2002**, *129*, 181–190.
(13) Amador, V.; Monte, E.; Garcia-Martinez, J. L.; Prat, S. Gibberellins signal nuclear import of PHOR*1*, a photoperiod-responsive protein with homology to Drosophila armadillo. *Cell* **2001**, *106*, 343–354.
(14) Fukazawa, J.; Sakai, T.; Ishida, S.; Yamaguchi, I.; Kamiya, Y.; Takahashi, Y. Repression of shoot growth, a bZIP transcriptional activator, regulates cell elongation by controlling the level of gibberellins. *Plant Cell* **2000**, *12*, 901–915.
(15) Ueguchi-Tanaka, M.; Ashikari, M.; Nakajima, M.; Itoh, H.; Katoh, E.; Kobayashi, M.; Chow, T. Y.; Hsing, Y. I.; Kitano, H.; Yamaguchi, I.; Matsuoka, M. GIBBERELLIN INSENSITIVE DWARF1 encodes a soluble receptor for gibberellin. *Nature* **2005**, *437*, 693–698.
(16) Ueguchi-Tanaka, M.; Fujisawa, Y.; Kobayashi, M.; Ashikari, M.; Iwasaki, Y.; Kitano, H.; Matsuoka, M. Rice dwarf mutant d1, which is defective in the alpha subunit of the heterotrimeric G protein, affects gibberellin signal transduction. *Proc. Natl. Acad. Sci. U.S.A.* **2000**, *97*, 11638–11643.
(17) Ueguchi-Tanaka, M.; Nakajima, M.; Motoyuki, A.; Matsuoka, M. Gibberellin receptor and its role in gibberellin signaling in plants. *Annu. Rev. Plant Biol.* **2007**, *58*, 183–198.
(18) McGinnis, K. M.; Thomas, S. G.; Soule, J. D.; Strader, L. C.; Zale, J. M.; Sun, T. P.; Steber, C. M. The Arabidopsis SLEEPY1 gene encodes a putative F-box subunit of an SCF E3 ubiquitin ligase. *Plant Cell* **2003**, *15*, 1120–1130.
(19) Sasaki, A.; Itoh, H.; Gomi, K.; Ueguchi-Tanaka, M.; Ishiyama, K.; Kobayashi, M.; Jeong, D. H.; An, G.; Kitano, H.; Ashikari, M.; Matsuoka, M. Accumulation of phosphorylated repressor for gibberellin signaling in an F-box mutant. *Science* **2003**, *299*, 1896–1898.
(20) Galat, A. Variations of sequences and amino acid compositions of proteins that sustain their biological functions: An analysis of the cyclophilin family of proteins. *Arch. Biochem. Biophys.* **1999**, *371*, 149–162.
(21) Romano, P. G.; Horton, P.; Gray, J. E. The Arabidopsis cyclophilin gene family. *Plant Physiol.* **2004**, *134*, 1268–1282.
(22) Gasser, C. S.; Gunning, D. A.; Budelier, K. A.; Brown, S. M. Structure and expression of cytosolic cyclophilin/peptidyl-prolyl cis-trans isomerase of higher plants and production of active tomato cyclophilin in Escherichia coli. *Proc. Natl. Acad. Sci. U.S.A.* **1990**, *87*, 9519–9523.
(23) Edvardsson, A.; Eshaghi, S.; Vener, A. V.; Andersson, B. The major peptidyl-prolyl isomerase activity in thylakoid lumen of plant chloroplasts belongs to a novel cyclophilin TLP20. *FEBS Lett.* **2003**, *542*, 137–141.
(24) Fulgosi, H.; Vener, A. V.; Altschmied, L.; Herrmann, R. G.; Andersson, B. A novel multi-functional chloroplast protein: identification of a 40 kDa immunophilin-like protein located in the thylakoid lumen. *Embo J.* **1998**, *17*, 1577–1587.
(25) Vener, A. V.; Rokka, A.; Fulgosi, H.; Andersson, B.; Herrmann, R. G. A cyclophilin-regulated PP2A-like protein phosphatase in thylakoid membranes of plant chloroplasts. *Biochemistry* **1999**, *38*, 14955–14965.
(26) Geisler, M.; Kolukisaoglu, H. U.; Bouchard, R.; Billion, K.; Berger, J.; Saal, B.; Frangne, N.; Koncz-Kalman, Z.; Koncz, C.; Dudler, R.; Blakeslee, J. J.; Murphy, A. S.; Martinoia, E.; Schulz, B. TWISTED DWARF1, a unique plasma membrane-anchored immunophilin-like protein, interacts with Arabidopsis multidrug resistance-like transporters AtPGP1 and AtPGP19. *Mol. Biol. Cell* **2003**, *14*, 4238–4249.
(27) Berardini, T. Z.; Bollman, K.; Sun, H.; Poethig, R. S. Regulation of vegetative phase change in Arabidopsis thaliana by cyclophilin 40. *Science* **2001**, *291*, 2405–2407.
(28) Faure, J. D.; Vittorioso, P.; Santoni, V.; Fraisier, V.; Prinsen, E.; Barlier, I.; Van Onckelen, H.; Caboche, M.; Bellini, C. The PASTICCINO genes of Arabidopsis thaliana are involved in the control of cell division and differentiation. *Development* **1998**, *125*, 909–918.
(29) Li, H.; He, Z.; Lu, G.; Lee, S. C.; Alonso, J.; Ecker, J. R.; Luan, S. A WD40 domain cyclophilin interacts with histone H3 and functions in gene repression and organogenesis in Arabidopsis. *Plant Cell* **2007**, *19*, 2403–2416.
(30) Chong, K.; Bao, S. L.; Xu, T.; Liang, T. B.; Huang, H. L.; Zeng, J. Z.; Xu, J.; Xu, Z. H. Functional analysis of ver gene using antisense transgenic wheat plant. *Physiol. Plant.* **1998**, *102*, 87–92.
(31) Abraham, E.; Rigo, G.; Szekely, G.; Nagy, R.; Koncz, C.; Szabados, L. Light-dependent induction of proline biosynthesis by abscisic acid and salt stress is inhibited by brassinosteroid in Arabidopsis. *Plant Mol. Biol.* **2003**, *51*, 363–372.
(32) Botwright, T. L.; Rebetzke, G. J.; Condon, A. G.; Richards, R. A. Influence of the gibberellin-sensitive Rht8 dwarfing gene on leaf epidermal cell dimensions and early vigour in wheat (Triticum aestivum L.). *Ann. Bot. (London)* **2005**, *95*, 631–639.
(33) Laemmli, U. K. Cleavage of structural proteins during the assembly of the head of bacteriophage T4. *Nature* **1970**, *227*, 680–685.
(34) Qin, G.; Tian, S.; Chan, Z.; Li, B. Crucial role of antioxidant proteins and hydrolytic enzymes in pathogenicity of Penicillium expansum: analysis based on proteomics approach. *Mol. Cell. Proteomics* **2007**, *6*, 425–438.
(35) Jilkina, O.; Bhullar, R. P. Generation of antibodies specific for the RalA and RalB GTP-binding proteins and determination of their concentration and distribution in human platelets. *Biochim. Biophys. Acta* **1996**, *1314*, 157–166.
(36) Clough, S. J.; Bent, A. F. Floral dip: a simplified method for Agrobacterium-mediated transformation of Arabidopsis thaliana. *Plant J.* **1998**, *16*, 735–743.
(37) Supartana, P.; Shimizu, T.; Nogawa, M.; Shioiri, H.; Nakajima, T.; Haramoto, N.; Nozue, M.; Kojima, M. Development of simple and efficient in Planta transformation method for wheat (Triticum aestivum L.) using Agrobacterium tumefaciens. *J. Biosci. Bioeng.* **2006**, *102*, 162–170.
(38) Xu, Y. L.; Li, L.; Wu, K.; Peeters, A. J.; Gage, D. A.; Zeevaart, J. A. The GA5 locus of Arabidopsis thaliana encodes a multifunctional gibberellin 20-oxidase: molecular cloning and functional expression. *Proc. Natl. Acad. Sci. U.S.A.* **1995**, *92*, 6640–6644.
(39) Arevalo-Rodriguez, M.; Wu, X.; Hanes, S. D.; Heitman, J. Prolyl isomerases in yeast. *Front. Biosci.* **2004**, *9*, 2420–2446.
(40) Marks, A. R. Cellular functions of immunophilins. *Physiol. Rev.* **1996**, *76*, 631–649.
(41) Keyes, G.; Sorrells, M. E.; Setter, T. L. Gibberellic Acid Regulates Cell Wall Extensibility in Wheat (Triticum aestivum L.). *Plant Physiol.* **1990**, *92*, 242–245.
(42) Hedden, P.; Kamiya, Y. GIBBERELLIN BIOSYNTHESIS: Enzymes, Genes and Their Regulation. *Annu. Rev. Plant Physiol. Plant Mol. Biol.* **1997**, *48*, 431–460.
(43) Kaneko, M.; Itoh, H.; Ueguchi-Tanaka, M.; Ashikari, M.; Matsuoka, M. The alpha-amylase induction in endosperm during rice seed germination is caused by gibberellin synthesized in epithelium. *Plant Physiol.* **2002**, *128*, 1264–1270.
(44) Liu, J.; Chen, C. M.; Walsh, C. T. Human and Escherichia coli cyclophilins: sensitivity to inhibition by the immunosuppressant cyclosporin A correlates with a specific tryptophan residue. *Biochemistry* **1991**, *30*, 2306–2310.
(45) Zydowsky, L. D.; Etzkorn, F. A.; Chang, H. Y.; Ferguson, S. B.; Stolz, L. A.; Ho, S. I.; Walsh, C. T. Active site mutants of human cyclophilin A separate peptidyl-prolyl isomerase activity from cyclosporin A binding and calcineurin inhibition. *Protein Sci.* **1992**, *1*, 1092–1099.
(46) Ivanchenko, M. G.; Coffeen, W. C.; Lomax, T. L.; Dubrovsky, J. G. Mutations in the Diageotropica (Dgt) gene uncouple patterned cell division during lateral root initiation from proliferative cell division in the pericycle. *Plant J.* **2006**, *46*, 436–447.
(47) Bouchard, R.; Bailly, A.; Blakeslee, J. J.; Oehring, S. C.; Vincenzetti, V.; Lee, O. R.; Paponov, I.; Palme, K.; Mancuso, S.; Murphy, A. S.; Schulz, B.; Geisler, M. Immunophilin-like TWISTED DWARF1 modulates auxin efflux activities of Arabidopsis P-glycoproteins. *J. Biol. Chem.* **2006**, *281*, 30603–30612.
(48) Kurek, I.; Aviezer, K.; Erel, N.; Herman, E.; Breiman, A. The wheat peptidyl prolyl cis-trans-isomerase FKBP77 is heat induced and developmentally regulated. *Plant Physiol.* **1999**, *119*, 693–704.
(49) Yi, H.; Friedman, J. L.; Ferreira, P. A. The cyclophilin-like domain of Ran-binding protein-2 modulates selectively the activity of the ubiquitin-proteasome system and protein biogenesis. *J. Biol. Chem.* **2007**, *282*, 34770–34778.

PR100560V